Polymer Chemistry

Hydrolytically-Degradable Homo- and Copolymers of a Strained Exocyclic Hemiacetal Ester

Journal:	*Polymer Chemistry*
Manuscript ID	PY-ART-05-2019-000797.R1
Article Type:	Paper
Date Submitted by the Author:	15-Jul-2019
Complete List of Authors:	Neitzel, Angelika; University of Chicago, Institute for Molecular Engineering Barreda, Leonel; University of Minnesota Twin Cities, Chemistry Trotta, Jacob; Cornell University, Chemistry and Chemical Biology Fahnhorst, Grant; University of Minnesota Twin Cities, Chemistry Haversang, Thomas; University of Minnesota Twin Cities Hoye, T.; University of Minnesota, Chemistry Fors, Brett; Cornell University, Department of Chemistry and Chemical Biology Hillmyer, Marc; University of Minnesota, Chemistry

Hydrolytically-Degradable Homo- and Copolymers of a Strained Exocyclic Hemiacetal Ester

Angelika E. Neitzel,[†] Leonel Barreda,[‡] Jacob T. Trotta,[§] Grant W. Fahnhorst,[‡] Thomas J. Haversang,[†] Thomas R. Hoye,[‡] Brett P. Fors,[§,] Marc A. Hillmyer[‡,*]*

[†]Department of Chemical Engineering and Materials Science, and [‡]Department of Chemistry University of Minnesota, Minneapolis, MN 55455-0431

[§]Department of Chemistry and Chemical Biology, Cornell University, Ithaca, NY 14853

*Corresponding author (e-mail: hillmyer@umn.edu, bpf46@cornell.edu)

Abstract

We report the cationic ring-opening homo- and copolymerization of the 7-membered exocyclic hemiacetal ester 7-methoxyoxepan-2-one (MOPO) to afford poly(7-methoxyoxepan-2-one) [poly(MOPO)] and its copolymers with isobutyl vinyl ether (IBVE) that achieve essentially quantitative conversions of 7-methoxyoxepan-2-one. The amorphous homopolymer is characterized by a low glass transition temperature of $T_g = -37$ ºC and is readily degraded under both acidic and basic conditions at the labile acylacetal linkages. With triflic acid as the cationic initiator the homopolymerization proceeds by an uncontrolled active chain end mechanism to reproducibly yield poly(MOPO) of M_n ~20 kg/mol. The monomer was also polymerized by a photoinitiated process using a dithiocarbamate or trithiocarbonate chain transfer agent and the photocatalyst 2,4,6-tris(*p*-4-methoxyphenyl)pyrylium tetrafluoroborate. Lower molar mass polymers were recovered at high initial concentrations of dithiocarbamate as compared to no chain transfer agent, indicating some ability to control polymer molar mass. Photoinitiated copolymerization of MOPO and IBVE afforded a tapered copolymer with MOPO-MOPO, IBVE-MOPO, and IBVE-IBVE linkages that degraded into low molar mass poly(IBVE) fragments in hydrochloric acid through hydrolysis of the acylacetal linkages resulting from ring-opened MOPO units in the backbone.

Introduction

The municipal solid waste stream (MSW) in the United States contained approximately 13% plastic materials by weight in 2013.[1] The largest contributor to plastic waste was identified as plastic packaging, which constitutes 26% of the total plastic in the MSW by volume.[2] Recently, the Ellen MacArthur foundation estimated that 40 billion USD are lost annually in addressing leakage of these lightweight materials into the environment.[2] The economic and environmental repercussions of the current plastics dilemma has motivated numerous approaches to minimize plastic waste. One interesting avenue is the controlled polymerization of monomers containing hydrolytically sensitive linkages to tailor water-mediated degradation profiles of plastics. In line with this goal, we have explored the ring-opening polymerization of cyclic hemiacetal esters to afford polymers bearing labile acylacetal linkages.

Previously we reported the ring-opening polymerization (ROP) of 2-methyl-1,3-dioxan-4-one (MDO) using diethylzinc (Et_2Zn)[3] or diphenylphosphoric acid (DPP)[4] catalyst with alcohol initiators (ROH, Scheme 1**a**,**b**). We found that MDO can undergo polymerization by two competing mechanisms: (a) activated monomer, leading to poly(2-methyl-1,3-dioxan-4-one) [poly(MDO)] via ring-opening at the acetal functionality, and (b) coordination-insertion, proceeding via ring-opening at the ester group with concurrent expulsion of acetaldehyde to yield poly(3-hydroxypropionic acid) [poly(3-HPA)]. The latter polymerization, driven by the loss of volatile byproduct, was consequently optimized, expanded and improved in the polymerization of substituted 1,3-dioxolan-4-ones (DOLOs). Notably, this allowed for the straightforward production of poly(mandelic acid) with control over tacticity (Scheme 1**d**).[5,6]

Aoshima and coworkers recently showed that, unlike MDO, unstrained DOLOs do not undergo homopolymerization under cationic ROP conditions. However, the thermodynamics can be favorably shifted to enable their co- and terpolymerization with oxiranes and

oxiranes/vinyl ethers, respectively (Scheme 1**c**).[7] The reluctance of DOLOs to polymerize to the corresponding poly(hemiacetal esters) is in good agreement with what was previously determined computationally for the parent compound 1,3-dioxolan-4-one (DOX) and what is well-known for γ-butyrolactone.[8,9] Consequently, despite reports to the contrary,[8] the co- and terpolymers do not feature any significant level of acylacetal linkages in the backbone because this would require sequential DOLO additions. Regardless, the co- and terpolymers could be readily degraded in weakly acidic conditions via hydrolysis at the acetal linkages arising from sequential DOLO/oxirane additions.

Scheme 1. Previous ring-opening polymerizations of cyclic hemiacetal esters

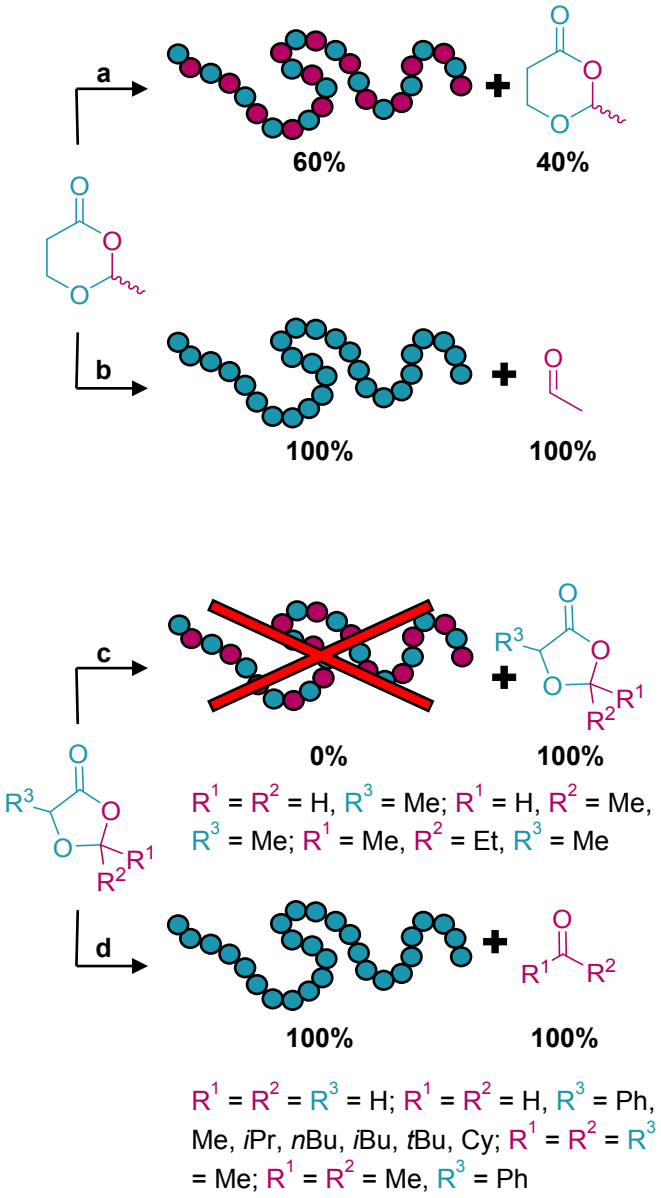

a. ROP of MDO to poly(MDO) with $[Et_2Zn]_0$ <14 mM[3] or DPP[4] and ROH initiators. **b.** ROP of MDO to poly(3-HPA) with $[Et_2Zn]_0$ ≥100 mM and ROH initiators via concurrent acetaldehyde extrusion.[3] **c**. No homopolymerization occurs in the attempted cationic ROP of 1,3-dioxolanones with tris(pentafluorophenyl)borane $[B(C_6F_5)_3]$.[7] **d.** ROP of 1,3-dioxolanones to polyesters with aluminum salen catalyst.[5]

We focused our efforts on the polymerization of 7-membered cyclic hemiacetal esters with the intent to capitalize on what we expected to be favorable ROP thermodynamics. We previously found that expanding MDO by a methylene unit to its unprecedented 7-membered ring analogues, incorporating either formaldehyde or acetaldehyde as the acetal component, afforded highly reactive monomers, which were unfortunately difficult to isolate without concurrent auto-polymerization or formation of the thermodynamically stable γ-butyrolactone via extrusion of aldehyde.[10] These findings motivated this investigation into the polymerization of the known exocyclic hemiacetal ester 7-methoxyoxepan-2-one (MOPO), which we hypothesized would not liberate volatile aldehyde during its polymerization due to the exocyclic placement of the acetal oxygen. In previous works MOPO has been employed as an initiator in the ring-expansion cationic homopolymerization of vinyl ethers affording cyclic polyvinyl ethers.[11-13] In this work we report the homo- and copolymerization of MOPO and our attempts to control its cationic ROP by reversible deactivation polymerization (RDP) methods (Scheme 2).

Scheme 2. MOPO homo- and copolymerization with IBVE to afford hydrolytically degradable poly(MOPO) and poly(MOPO-*co*-IBVE)

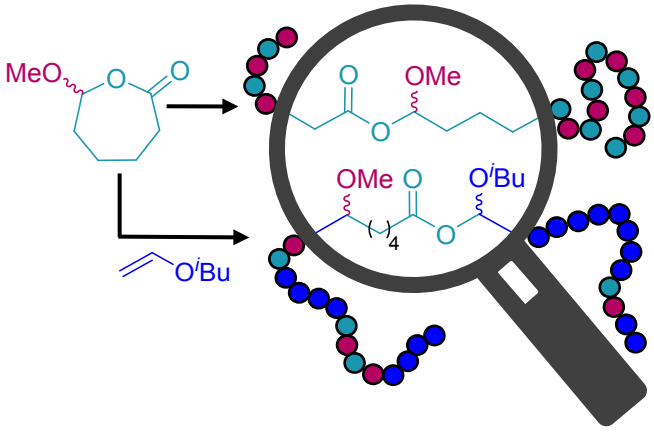

Results and Discussion

Monomer Synthesis. An attractive feature of MOPO is that its precursor 2-methoxycyclohexanone (**2**) can be sourced from guaiacol (**1**), a compound accessed from the hydrolysis or pyrolysis of lignin.[14] Guaiacol has previously been hydrogenated to 2-methoxycyclohexanol,[15] which can be oxidized to afford **2** (Scheme 3). We performed the Baeyer-Villiger oxidation of commercially available **2** as reported previously and obtained MOPO with essentially perfect regioselectivity.[11] The crude monomer could be purified by either flash column chromatography using base-treated silica or Kugelrohr distillation from calcium hydride onto a polystyrene matrix crosslinked with 2% divinylbenzene and 3.0 mmol/g bound 4-dimethylaminopyridine [poly(DMAP)]. We note that MOPO is highly reactive and readily auto-polymerizes upon contact with untreated glass surfaces, as well as hydrolyzes to 6-oxohexanoic acid and methanol in the presence of water (Figures S1–S3). Therefore, purified MOPO was stored over poly(DMAP) at –20 °C in a glovebox freezer. The high purity of MOPO (> 99%) was verified using gas chromatography-mass spectrometry (GC-MS) as well as proton and carbon nuclear magnetic resonance (^{1}H and ^{13}C NMR) spectroscopy prior to intentional polymerization (Figures S4–S6).

Scheme 3. Proposed synthesis of 7-methoxyoxepan-2-one from lignin

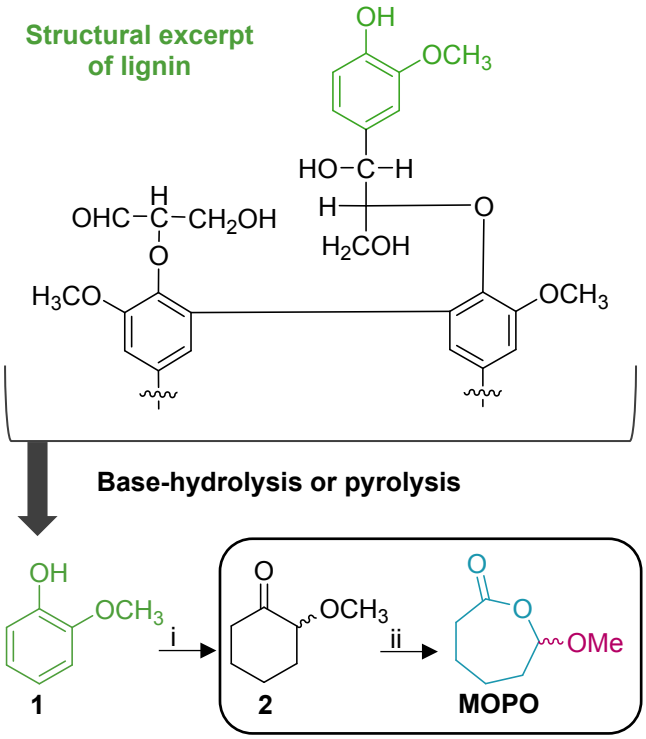

i) Hydrogenation/oxidation (not performed in this study). ii) *m*CPBA, DCM, 0 – 10 °C (68% purified yield).

Cationic ring-opening polymerization. In our initial studies we used anhydrous hydrochloric acid (HCl) in diethyl ether as catalyst and benzyl alcohol (BnOH) as an initiator to promote polymerization of MOPO. Poly(MOPO) synthesized in the bulk at room temperature with $[MOPO]_0/[BnOH]_0/[HCl]_0 = 500/10/1$ featured predominantly benzyl acetal end groups, most likely derived from reaction of an activated chain end with benzyl alcohol (Figure 1). End group analysis by ^{1}H NMR spectroscopy, assuming one end group per chain, gave a number-average molar mass of $M_{n,NMR}$ = 9.2 kg/mol ($M_{n,theo}$ = 4.3 kg/mol at 60% conversion) as compared to $M_{n,SEC}$ = 8.6 kg/mol and a dispersity of $Đ$ = 1.7 obtained from molar mass analysis by size exclusion chromatography (SEC) using chloroform ($CHCl_3$) as the eluent and polystyrene (PS) calibration standards (Figure S7). Thermal analysis of the purified poly(MOPO) indicated a thermal degradation temperature at 5% mass loss of $T_{d,95}$ = 175 °C and a glass transition temperature of T_g = −37 °C (Figures S8–S9).

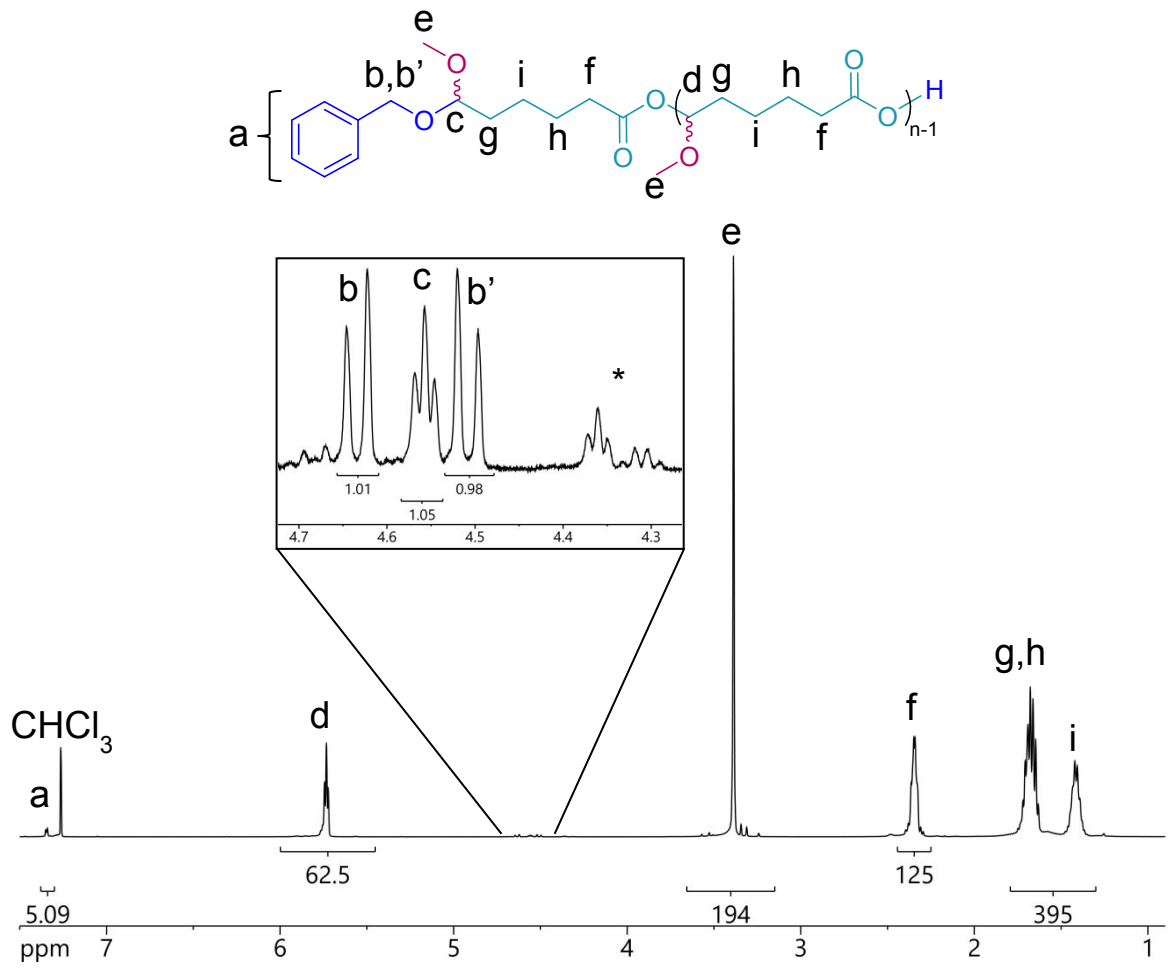

Figure 1. ^{1}H NMR ($CDCl_3$) spectrum of purified poly(MOPO) synthesized with HCl and BnOH (neat polymerization with $[MOPO]_0/[HCl]_0$ = 500 and $[MOPO]_0/[BnOH]_0$ = 50). By end group analysis $M_{n,NMR}$ = 9.2 kg/mol and by $CHCl_3$ SEC analysis relative to PS standards $M_{n,SEC}$ = 8.7 kg/mol and $Đ$ = 1.7. The signals marked * are attributed to enol ether end groups derived from deprotonation of a propagating alkoxycarbenium ion (c.f. Figure S10).

Polymerizations conducted under identical conditions but without exogenous benzyl alcohol initiator, yielded poly(MOPO) with a mixture of E- and Z-enol ether end groups **5**, presumably arising from elimination of the proton vicinal to the alkoxycarbenium ion **4** on the propagating chain end by intermolecular chain transfer from polymer to monomer (Scheme 4, Figures S10–S11). Enol ether end groups were observed even in the presence of high $[BnOH]_0$, indicating that the polymerization proceeded predominantly by an active chain end (ACE) mechanism and that benzyl alcohol acted as a chain-transfer agent rather than an initiator (Figure 1). This was further supported by experiments with HCl and BnOH where $M_{n,SEC}$ of

poly(MOPO) was monitored as a function of monomer conversion, indicating that molar mass was effectively constant with increasing conversion (Figure S12). From these data, we concluded that poly(MOPO) chains grew predominantly by an uncontrolled ACE mechanism and terminated via proton transfer to MOPO, thereby initiating new chains throughout the polymerization, much like what is observed in other uncontrolled cationic polymerizations.[16]

Scheme 4. Pathways in the cationic ROP of MOPO by an active chain end mechanism[i]

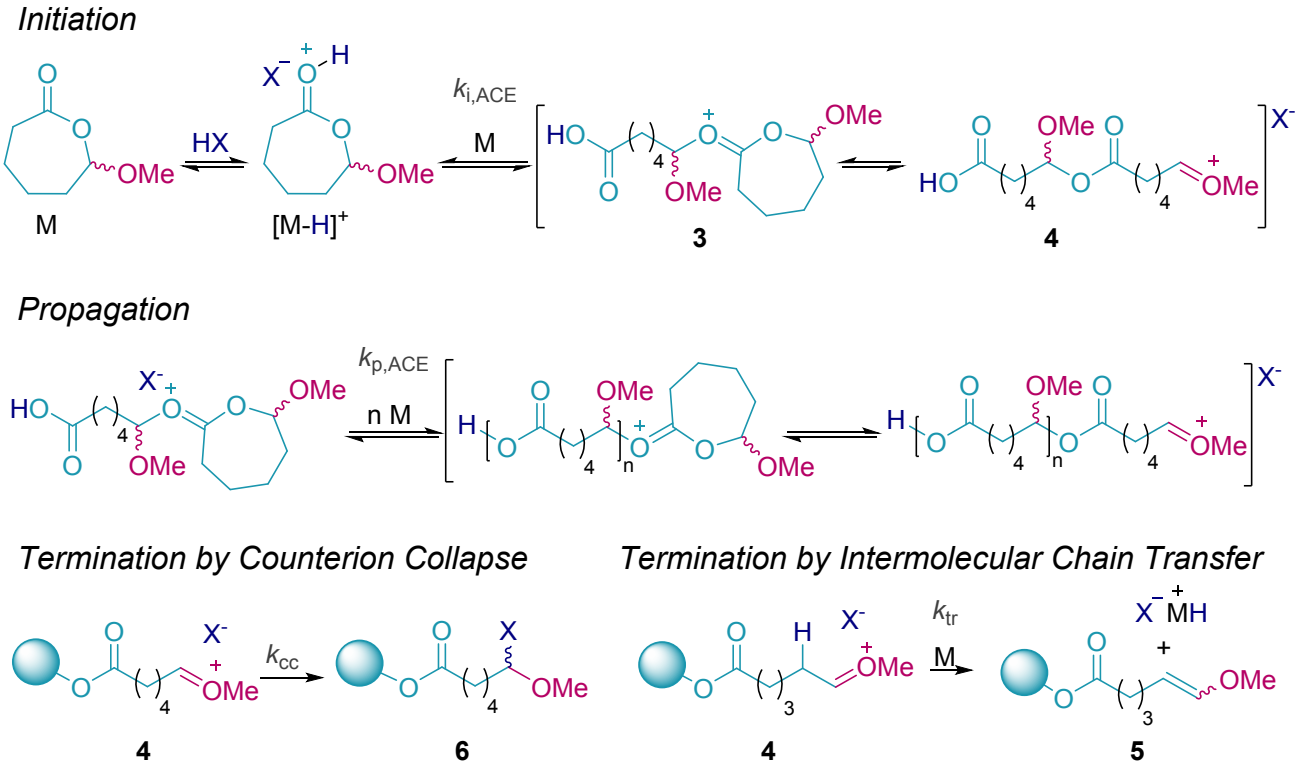

Even when polymerizations were performed neat, monomer conversions did not exceed 65% ($[MOPO]_0/[HCl]_0 = 500$, with $[MOPO]_0/[BnOH]_0 = 50$, or without exogenous initiator). Addition of more catalyst to a neat polymerization that had ceased at 60% increased the monomer conversion to 75%, which indicated that the catalyst became deactivated and that $[M]_{eq}$ had not yet been reached (Figure S13). In a separate solution polymerization of MOPO in $CDCl_3$ with higher loadings of HCl ($[MOPO]_0 = 1$ M, $[MOPO]_0/[HCl]_0 = 100$) we observed

[i] One may also envision stabilization of the propagating alkoxycarbenium ion **4** by a terminal carboxylate on poly(MOPO) as it was previously described for the ring-expansion cationic polymerization of vinyl ethers where MOPO was used as an initiator.[11]

a triplet at 5.45 ppm (J = 5 Hz) by ^{1}H NMR spectroscopy, in good agreement with previously reported ^{1}H NMR spectral shifts for methine protons in related 1-chloroalkyl methyl ethers (Figure S14).[17] This suggested that catalyst deactivation was, at least in part, attributable to the collapse of chloride anion onto the propagating alkoxycarbenium ion **4** to generate 1-chloroalkyl methyl ether **6** (Scheme 4). Further evidence for the presence of a propagating alkoxycarbenium ion was obtained by adding triphenylphosphine (PPh_3) to a solution polymerization of MOPO conducted with HCl. A new peak observed by phosphorous (^{31}P) NMR spectroscopy upon reaction of the propagating species with PPh_3 was in good agreement with the presence of a phosphonium ion, formed by addition of triphenylphosphine to a propagating alkoxycarbenium ion (Figure 2).[18,19]

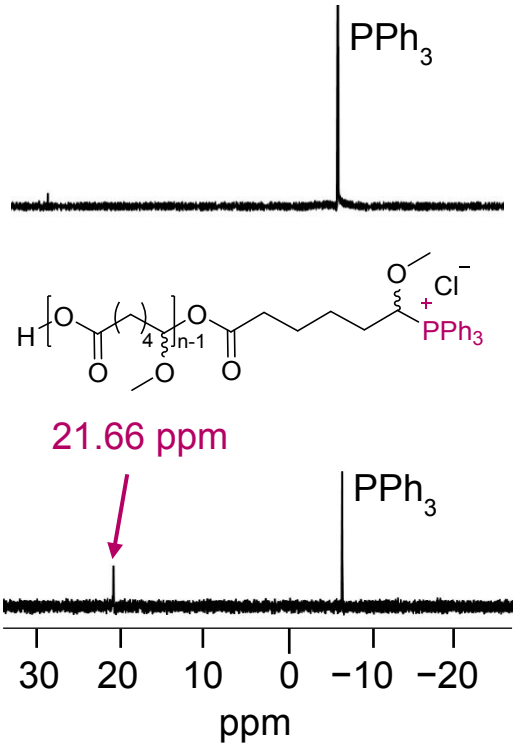

Figure 2. ^{31}P NMR ($CDCl_3$) spectra of recrystallized PPh_3 (top) and the adduct resulting from addition of PPh_3 to a solution polymerization of MOPO with HCl ($[MOPO]_0$ = 1 M in $CDCl_3$, $[MOPO]_0/[HCl]_0$ = 100).

In addition to the carboxylic acid and enol ether chain-ends observed by ^{1}H NMR spectroscopy, we also detected the formation of a small amount of aldehyde and (hemi)acetal.

Formation of aldehyde when treating MOPO with anhydrous HCl was not surprising, as hemiacetal esters have been implicated as intermediates in the acidolysis of acetals to aldehydes under water-free conditions.[20] To ensure that the aldehyde was not a poly(MOPO) chain end but rather resulted from a small amount of acidolysis of MOPO, we examined a sample containing poly(MOPO) and ca. 1% of the aldehyde contaminant in the presence of 4-nitrobenzaldehyde as a small molecule internal standard by diffusion-ordered (DOSY) NMR spectroscopy. The observed diffusion coefficient for the aldehyde contaminant was much closer in magnitude to the 4-nitrobenzaldehyde standard than the broad diffusion coefficient range associated with poly(MOPO) signals, convincing us that the aldehyde formed was present as a small molecule contaminant rather than a polymer chain end (Figure S15). We were able to identify the contaminants as 6-oxohexanoic acid[21] and its (hemi)acetal derivatives, compounds we previously observed during the intentional hydrolysis of MOPO in a mixture of acetonitrile and water (Figures S1–S3).

In an effort to suppress irreversible termination by counterion collapse, we exchanged HCl for methyl trifluoromethanesulfonate (methyl triflate, MeOTf). Triflate anion is a weaker nucleophile than chloride and is therefore less likely to irreversibly collapse onto the propagating alkoxycarbenium ion.[22] Polymerizations of MOPO with methyl triflate were carried out in $CDCl_3$ at –20 °C to mitigate transfer reactions. We were not able to further decrease the temperature because polymerization was too slow below –20 °C. Using $[MOPO]_0/[MeOTf]_0$ ~550 with $[MOPO]_0$ = 2.25 M, >95% conversion to poly(MOPO) was achieved in 1 h and poly(MOPO) of $M_{n,SEC}$ = 54 kg/mol and $Đ$ = 1.4 (determined by SEC with multiangle laser light scattering (MALLS) using dimethyl formamide as the eluent) was isolated by precipitation (Figure S16).

Encouraged by the high conversions of MOPO and high molar mass polymers achieved, we studied the polymerization of MOPO with MeOTf at −20 °C employing 3 different

monomer to catalyst ratios: $[MOPO]_0/[MeOTf]_0$ = 250, 500, and 1000. The polymerizations proceeded to >98% conversion and $CHCl_3$ SEC analysis of the crude polymerization mixtures indicated that poly(MOPO) of M_n ~19 kg/mol (relative to PS standards) was formed in all cases, irrespective of $[MeOTf]_0$ (Figure 3). From this result we concluded that, on one hand, the use of an initiator with a non-nucleophilic counterion mediated irreversible termination by counterion collapse; yet, on the other hand, facilitated transfer reactions as the propagating species was not stabilized by a reversibly associating counterion.

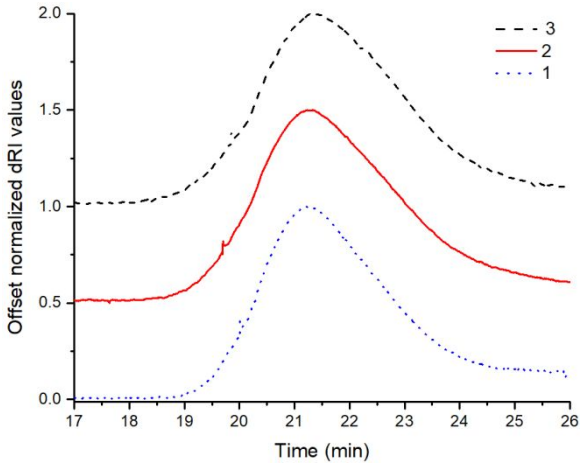

Figure 3. $CHCl_3$ SEC traces (flow rate = 1 mL/min) for poly(MOPO) synthesized with: 1) $[MOPO]_0/[MeOTf]_0$ = 250, 2) $[MOPO]_0/[MeOTf]_0$ = 500, and 3) $[MOPO]_0/[MeOTf]_0$ = 1000. In all cases poly(MOPO) of molar masses M_n ~19 kg/mol and $Đ$ = 1.8–2.1 were attained.

Because methyl triflate is a highly effective methylating agent,[23] we hypothesized that it would initiate polymerization by methylation of the MOPO ester carbonyl (Scheme 5). Upon monitoring the polymerization by ^1H and fluorine (^{19}F) NMR spectroscopy, we did not observe a trifluoromethyl ester end group on poly(MOPO) and did not detect consumption of methyl triflate at high monomer conversions. Analysis of our methyl triflate stock solution by ^{19}F NMR spectroscopy revealed the presence of a low concentration of triflic acid (TfOH). The triflic acid signal in the ^{19}F NMR spectrum was observed to shift with addition of monomer, suggesting that initiation of MOPO was promoted by proton transfer from triflic acid rather than by methyl transfer from MeOTf (Figures S17–S18).

Scheme 5. Polymerization of MOPO catalyzed by TfOH/MeOTf

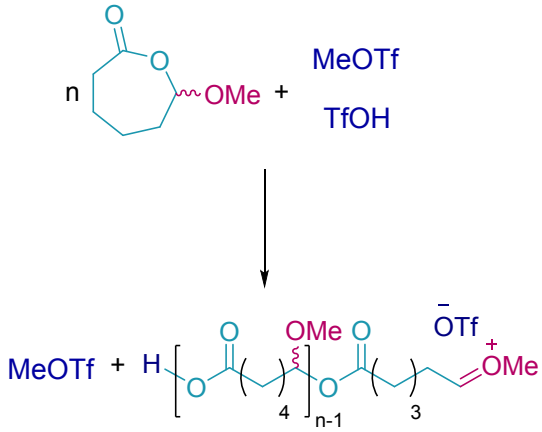

We estimated the concentration of triflic acid in our methyl triflate stock solution to be ca. 0.6% as determined by ^{19}F NMR spectroscopy using long relaxation delays (d_1 = 30 s). This translates to a $[MOPO]_0/[TfOH]_0$ ~80,000 when employing $[MOPO]_0/[MeOTf]_0$ ~500, consistent with remarkably low amounts of triflic acid being sufficient to initiate the polymerization. We thus tried to promote the polymerization with a stock solution of triflic acid in $CDCl_3$. Addition of low amounts of triflic acid ($[MOPO]_0/[TfOH]_0$ ~5,000 or 9,000, $[MOPO]_0$ = 2 M) afforded visibly viscous solutions over the course of 5 min and when quenched after 50 min MOPO conversions were 86% and 96%, respectively. Poly(MOPO) molar mass was higher and $Đ$ lower in the case of the lower $[TfOH]_0$ (for $[MOPO]_0/[TfOH]_0$ ~ 5,000: $M_{n,SEC\text{-}MALLS}$ = 23 kg/mol and $Đ$ = 2.1; for $[MOPO]_0/[TfOH]_0$ ~ 9,000: $M_{n,SEC\text{-}MALLS}$ = 63 kg/mol and $Đ$ = 1.7, Figure S19). When higher loadings of triflic acid stock solution ($[MOPO]_0/[TfOH]_0$ ~ 600) were used, the monomer violently decomposed to 6-oxohexanoic acid, its hemiacetal derivatives, and methanol (Figure S20). From these results we concluded that initiation of MOPO polymerization by strong protic acid is highly efficient and we had no clear evidence of initiation via an alkylation pathway.

To determine the highest molar mass of poly(MOPO) accessible through TfOH initiation, we carried out multiple MOPO polymerizations using the same monomer batch throughout and using varying $[MOPO]_0/[TfOH]_0$ ratios (5,000, 9,000, and 16,000). Working

with a single monomer batch was imperative because these cationic polymerizations are highly sensitive to low levels of impurities and, therefore, misleading trends may be deduced when comparing results across different monomer batches.[16] Table 1 lists results for polymerizations with conversions > 75%. Poly(MOPO) of $M_{n,SEC\text{-}MALLS}$ = 19 ± 5 kg/mol (mean of all entries in Table 2 ± 1 standard deviation, standard error = 1.22) was obtained regardless of $[TfOH]_0$. The variability in achievable molar mass as a function of monomer batch purity is evident from the lower molar mass polymers recovered from this batch as compared to the poly(MOPO) of M_n ~63 kg/mol obtained in initial experiments with TfOH using a distinct monomer batch. From the data in Table 1 we concluded that poly(MOPO) of M_n ~20 kg/mol can be reproducibly obtained with this monomer batch when promoting the polymerization at 2.25 M in $CDCl_3$ at –20 °C with [TfOH] ~9 ppm (entries 6–11, Table 1, mean M_n = 22 ± 4 kg/mol, standard error = 1.43).

Table 1. Polymerization of MOPO with ppm amounts of triflic acid.

Entry	$[MOPO]_0/[TfOH]_0$ (x 10^3)	Conversion[a] (%)	M_n[b] (kg/mol)	$Đ$[b]
1	5	95	15.2	1.28
2	5	94	12.3	1.61
3	5	84	15.8	1.39
4	5	90	19.0	1.28
5	5	87	20.2	1.41
6	9	83	20.2	1.41
7	9	85	25.6	1.35
8	9	86	26.7	1.38
9	9	77	22.0	1.29
10	9	94	18.3	1.41
11	9	96	18.9	1.30
12	16	83	26.2	1.33
13	16	93	13.4	1.51
14	16	90	17.1	1.40

All polymerizations were carried out in $CDCl_3$ distilled from P_2O_5 at $[MOPO]_0$ = 2.25 M and −20 °C in a glovebox for up to 1 h. Polymerizations were quenched with 1 μL of $[NaOPh]_{CDCl3}$ = 43 mM and precipitated into cold 9/1 hexanes/THF. TfOH was added as a 20 mM solution in $CDCl_3$ using a microsyringe. [a]Determined by ^1H NMR spectroscopy from relative integrations of monomer and polymer methine hydrogens geminal to the methyl ether. [b]Determined by DMF SEC-MALLS using d*n*/d*c*[poly(MOPO)] = 0.029.

Poly(MOPO) synthesis under reversible deactivation polymerization (RDP) conditions. We showed that the propagating species in MOPO polymerization with a cationic

initiator is alkoxycarbenium **4** (presumably in equilibrium with dioxocarbenium ion **3**), which we were able to trap experimentally (Figure 2, Scheme 4). Alkoxycarbenium **4** is identical to the propagating species in the cationic polymerization of vinyl ethers.[24] Over the past decades a variety of methods to control cationic polymerizations of vinyl ethers have emerged, including sulfide-mediated[25] (dissociation-combination), Lewis acid-catalyzed[26] (atom-transfer), and cationic reversible addition-fragmentation chain-transfer (RAFT, degenerative chain-transfer)[27] type RDPs (Scheme 6). We hypothesized that undesirable transfer and termination reactions occurring during MOPO polymerization could be mitigated by decreasing the concentration of propagating alkoxycarbenium centers via one of these approaches.

Scheme 6. Equilibria proposed for the reversible deactivation polymerization of MOPO

Sulfide-Mediated:

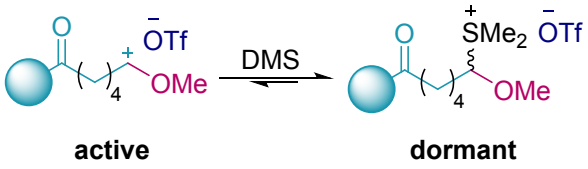

Lewis Acid-Catalyzed:

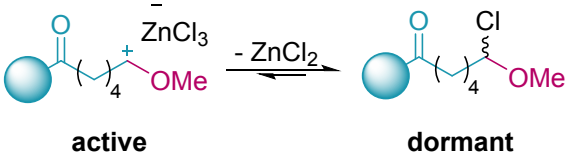

Degenerative Chain-Transfer:

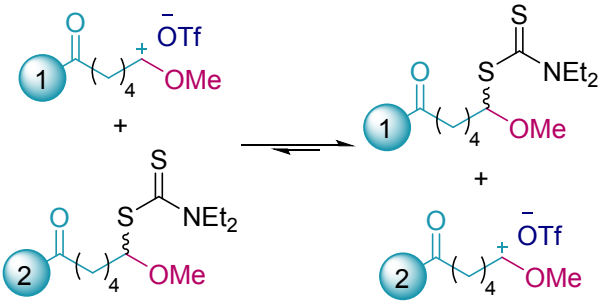

When performing MOPO polymerization in the presence of dimethyl sulfide (DMS) using methyl triflate as the cationogen source at −20 °C in $CDCl_3$, we observed a significant retardation of the polymerization rate ($[MOPO]_0/[DMS]_0/[MeOTf]_0$ = 500/100/1). However, when monitoring molar mass with conversion by $CHCl_3$ SEC, we did not observe an increase in molar mass with conversion, similar to our results from experiments conducted without DMS (Figure 4, c.f. Figure 3). From this we concluded that DMS did not form an adduct that efficiently suppressed transfer and termination events. Next, we probed the reactivation of the chloroalkyl methyl ether formed in the polymerization of MOPO with HCl by zinc chloride ($ZnCl_2$). This required that $ZnCl_2$ on its own would not promote polymerization of MOPO and only act according to Scheme 6 to revert chloride counter ion collapse. However, treatment of MOPO ($[MOPO]_0$ = 2.25 M in $CDCl_3$) with $ZnCl_2$ in diethyl ether resulted in the immediate

formation of poly(MOPO) when monitoring the polymerization by ^{1}H NMR spectroscopy (Figure S21). Careful optimization of sulfide-mediated and Lewis acid-catalyzed polymerization of MOPO may result in a more controlled system; however, this was not further investigated here.

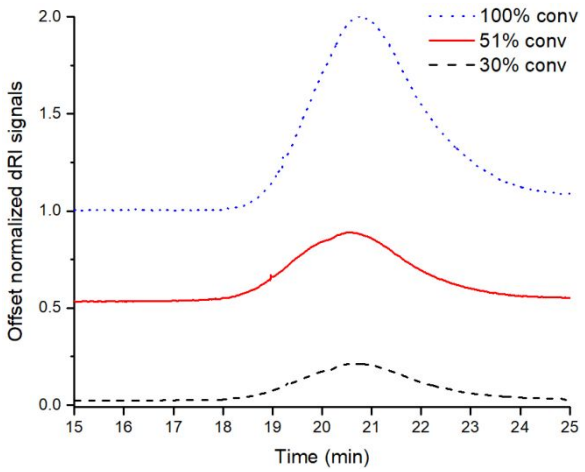

Figure 4. $CHCl_3$ SEC traces (flow rate = 1 mL/min) of poly(MOPO) molar mass evolution with conversion in the presence of DMS ($[MOPO]_0$ = 2.5 M in $CDCl_3$ at −20 °C with $[MOPO]_0/[MeOTf]_0$ = 500 and $[DMS]_0/[MeOTf]_0$ = 100). No linear increase in molar mass was observed with increasing conversion, although the rate of polymerization was significantly retarded.

Inspired by the control gained in the cationic RAFT polymerization of vinyl ethers recently developed by Kamigaito,[27-30] we proposed that the addition of a dithiocarbonyl chain-transfer agent (CTA) to the polymerization of MOPO could similarly promote a RAFT process to afford a controlled polymerization (Scheme 6). To test this, we synthesized diethyl dithiocarbamate **7**, trithiocarbonate **8**, and MOPO-based diethyl dithiocarbamate **9** (Figures S22–S23). We then probed the polymerization of MOPO under blue light irradiation using the photocatalyst 2,4,6-tris(*p*-4-methoxyphenyl)pyrylium tetrafluoroborate (**10**), previously used for the photo-controlled RAFT polymerization of vinyl ethers,[31,32] with **7**, **8**, or **9** as CTAs (Scheme 7 and Table 2).

Scheme 7. CTAs and catalyst used in the photomediated RAFT polymerization of MOPO

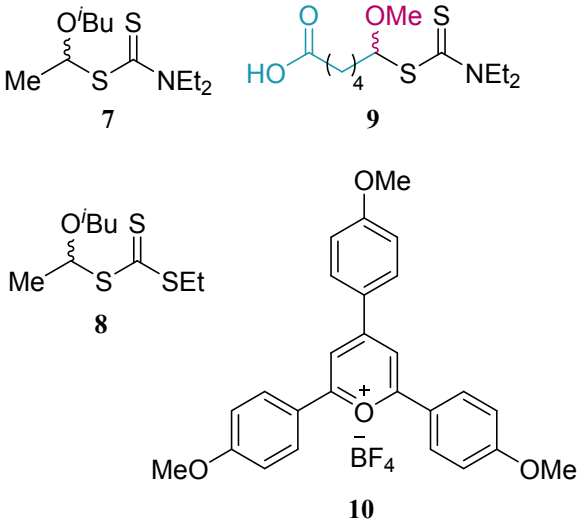

In the presence of CTAs **7**, **8**, or **9**, photocatalyst **10** converted 50 to 70% of MOPO to poly(MOPO) after exposure to blue light for 0.6 h to yield 7.2, 15.8, and 18.8 kg/mol polymers, respectively, with *Đ*s ranging from 1.8 to 2.3 (Table 2, entries 1–3, Figure S24). Using CTA **7**, we then varied the $[MOPO]_0/[CTA]_0$ ratio in an attempt to generate polymers of different molar masses. While at a 40/1 $[MOPO]_0/[CTA]_0$ ratio (Table 2, entry 2) we obtained a 7.2 kg/mol polymer, increasing $[MOPO]_0/[CTA]_0$ to 300/1 and 500/1 resulted in 20.7 and 31.8 kg/mol polymers, respectively, with dispersities between 1.8 and 2.1 observed in all cases (Figure 5). These results provide evidence that the polymerization is proceeding in part by the RAFT process and that varying the monomer to CTA ratio affords moderate control over M_n.

Table 2. Photomediated cationic RAFT polymerization of MOPO with various CTAs

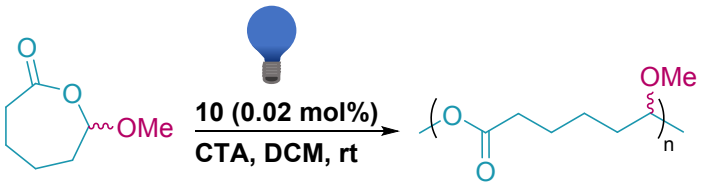

Entry	CTA	$[MOPO]_0/[CTA]_0$	Conversion[a] (%)	$M_{n,theo}$ [b] (kg/mol)	M_n [c] (kg/mol)	$Đ$[c]
1	**7**	40/1	52	2.7	7.2	1.79
2	**8**	40/1	51	3.2	15.8	1.91
3	**9**	40/1	67	4.4	18.8	2.30
4	**7**	300/1	88	37.0	20.7	2.11
5	**7**	500/1	93	66.4	31.8	1.85
6	None	-	99	-	36.8	2.30

[a]Polymerizations were run for between 0.1 and 0.6 h with $[MOPO]_0$ ~3 M in DCM. [b]Calculated from the $[MOPO]_0/[CTA]_0$ ratio and conversion. [c]Determined from THF SEC using polystyrene standards. All polymerizations were set up in an Unilab MBraun glovebox with a nitrogen atmosphere and irradiated with blue diode LED® BLAZE™ lights (450 nm, 2.88 W/ft) under nitrogen atmosphere outside the glovebox.

In the absence of any CTA, polymerization of MOPO resulted in a 36.8 kg/mol polymer with a dispersity of 2.3, indicating that photocatalyst **10** could also directly initiate MOPO polymerization through a putative monomer or solvent oxidation pathway. Additional experiments at lower temperatures (ca. −15 °C) in $CDCl_3$ did not result in improved control over the system, though the ability to generate different molar masses by varying $[MOPO]_0/[CTA]_0$ was retained (Figure S25).

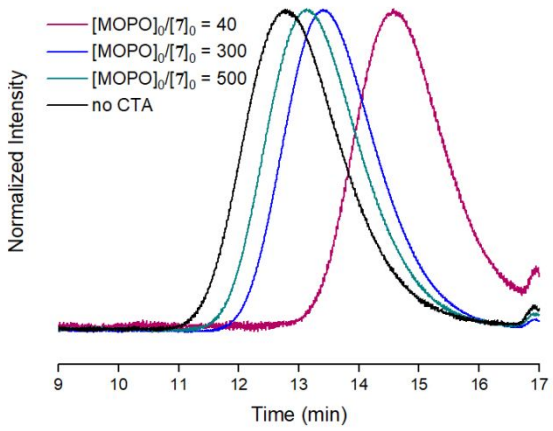

Figure 5. Refractive index chromatographs from THF SEC analysis of poly(MOPO) generated with different $[MOPO]_0$:$[\mathbf{7}]_0$ ratios from entries 1, 4, 5, and 6 in Table 2 (flow rate = 0.35 mL/min).

To further probe the photoinitiation in this system, we explored the relationship between photocatalyst **10** and MOPO through cyclic voltammetry (CV) and fluorescence quenching studies. The onset oxidation of CTA **7** is known to be +0.98 V (vs Ag/Ag^+). A CV of MOPO in DCM, the polymerization solvent, showed no oxidation below the solvent window (ca. + 2.5 V vs. Ag/Ag^+), indicating the onset oxidation for MOPO to be >+2.5 V (vs. Ag/Ag^+), significantly above **7**. This demonstrates that the CTA is much more readily oxidized than MOPO (Figures S26–S27). Additionally, at millimolar concentrations of MOPO, no fluorescence quenching of **10** by MOPO was observed, whereas appreciable fluorescence quenching of **10** by **7** is known,[6] indicating a higher quenching constant for **7** (Figures S28–S29). These results suggest that photoinitiation likely occurs by oxidation at **7** rather than MOPO (Scheme 8). In the absence of CTA, direct oxidation of MOPO or solvent by **10** (oxidation potential of +1.84 V vs SCE) likely leads to initiation.

Scheme 8. Putative mechanism of MOPO polymerization by photomediated cationic RAFT

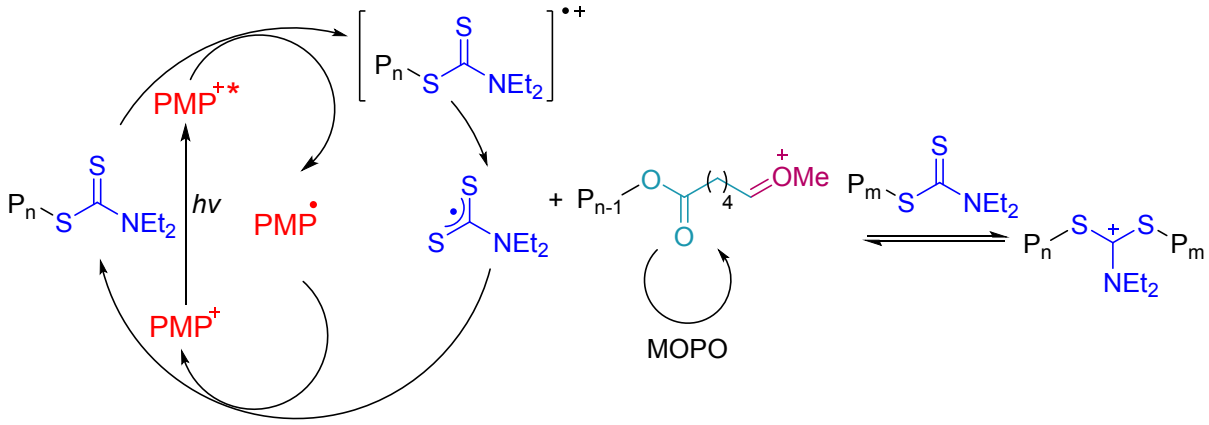

Photomediated cationic copolymerization of MOPO and isobutyl vinyl ether. To take advantage of the photo-mediated cationic polymerization, we performed copolymerizations of MOPO with IBVE to give readily degradable polymers (Scheme 9). Specifically, only the acylacetal units arising from incorporation of MOPO along the copolymer backbone are expected to undergo degradation upon acidic treatment, resulting in the controllable degradation of poly(MOPO-*co*-IBVE) to lower molar mass poly(IBVE)

fragments. From a 8 mol% MOPO and 92 mol% IBVE feed ($[MOPO+IBVE]_0/[\mathbf{7}]_0$ = 185), photocatalyst **10** converted 100% and 42% of MOPO and IBVE, respectively, after 3 h of blue light irradiation, resulting in a 9.3 kg/mol poly(MOPO-*co*-IBVE) sample with a dispersity of 1.48. ^{1}H and ^{13}C NMR spectral analysis of this polymer indicates 17 mol% MOPO incorporation into the copolymer from the initial 8 mol% MOPO feed, in excellent agreement with the 17 mol% MOPO incorporation obtained from the monomer conversions (Figures S30–S33).

Scheme 9. Photomediated RAFT copolymerization of MOPO and IBVE

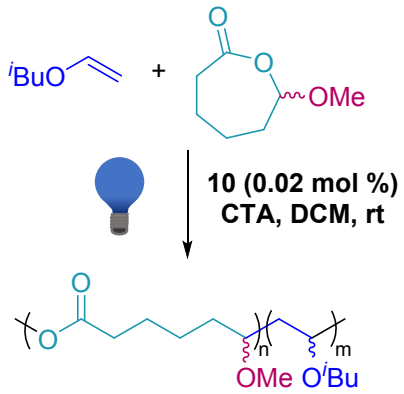

All polymerizations were set up in an Unilab MBraun glovebox with a nitrogen atmosphere and irradiated with blue diode LED® BLAZE™ lights (450 nm, 2.88 W/ft) under nitrogen atmosphere outside the glovebox.

2D ^{1}H NMR spectral assignments of poly(MOPO-*co*-IBVE) reveal two types of acylacetal resonances at ca. δ = 5.7 and 5.9 ppm that correspond to MOPO-MOPO and IBVE-MOPO linkages, respectively (Figures S34–S36). Integration of these resonances (Figure S30) indicate 62% MOPO-MOPO linkages and 38% IBVE-MOPO repeat units. A third, non-acylacetal linkage resulting from attack of IBVE onto MOPO, was also detected but could not be integrated due to overlapping peaks in the ^{1}H NMR spectrum (Scheme 9, Figures S34 – S36). The presence of IBVE-MOPO linkages suggests that MOPO and IBVE are incorporated into the same polymer backbone and that acid treatment of this material will selectively degrade the acylacetal linkages throughout the copolymer and give rise to lower molecular weight poly(IBVE).

Poly(MOPO) Degradation. We studied hydrolytic degradation of poly(MOPO), monitoring the changes using ^{1}H NMR spectroscopy. The cosolvent DMSO-d_6:H_2O (20:1) gave a homogeneous solution of poly(MOPO). To this was added a sufficient amount of either 2 M aqueous HCl or NaOH solution to bring the composition of the final mixture to 0.1 M in 10:1 DMSO-d_6:H_2O. Each of these degradation reaction mixtures remained homogenous. An initial ^{1}H NMR spectrum was recorded within 1 minute and several others at later time points (Figure S37).

Under acidic conditions, the degradation of each repeating acylacetal unit was fully cleaved to 6-oxohexanoic acid **11-H** and methanol, with a $t_{1/2}$ of ca. 5 minutes (Scheme 10). This conversion was characterized by i) the upfield shift of the -OCH_3 resonance from δ = 3.26 in poly(MOPO) to δ = 3.15 ppm and ii) the disappearance of the acylacetal methine proton (δ = 5.64 ppm) and accompanying growth of a resonance for an aldehyde proton (δ = 9.63 ppm). A few percent of the hydrated aldehyde was observed, as judged by a resonance at δ = 4.72 ppm. The cleavage of the benzyl acetal end group was much slower with a $t_{1/2}$ of ca. 1 hour.

Scheme 10. Degradation of poly(MOPO) in acidic and basic media

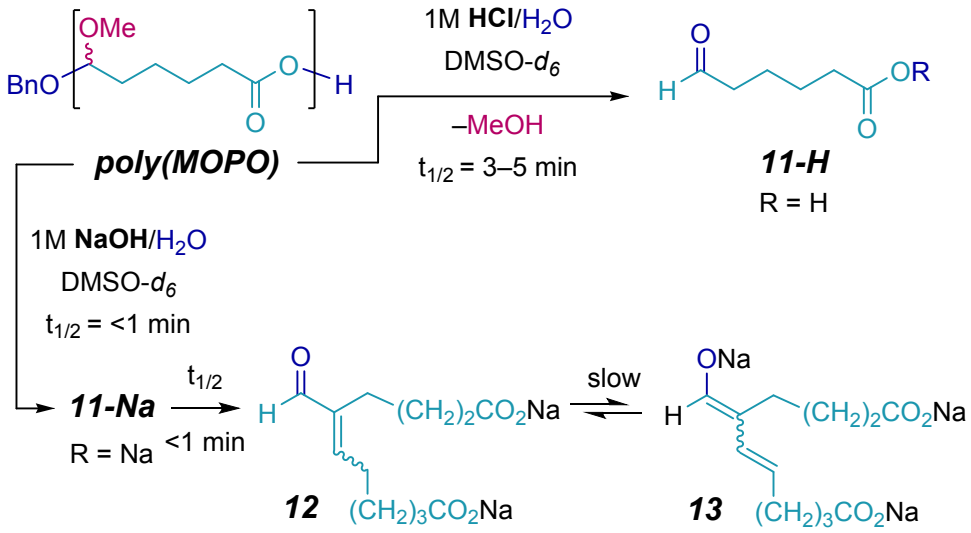

The base-induced degradation was more complicated. The following NMR spectral characteristics and peak assignments were guided vis-á-vis comparisons made for analogous

reaction mixtures starting with i) propionaldehyde and ii) 2-methylpentenal. The hemiacetal ester linkages in poly(MOPO) were fully degraded at the earliest time point ($t_{1/2}$ <1 min), and this sample already contained resonances associated with two aldehydes and several olefinic protons. We interpret this to mean that poly(MOPO) quickly degrades to **11-Na** [aldehyde triplet (J = 1.2 Hz) at δ = 8.79 ppm]. This aldehyde further, and rapidly, undergoes a self-aldol condensation reaction to give the enal **12** [aldehyde singlet at δ = 9.30[33] ppm and alkene triplet (J = 7.4 Hz) at δ = 6.59 ppm], which then slowly deprotonates to give the dienolate anion **13** [alkenes at δ = 7.00 (s), 5.67 (d, J = 15.1 Hz), and 4.48 (dt, J = 15.4, 6.5 Hz) ppm, see Figure S38 for mechanisms]. The chemical shifts and coupling constants of these resonances are very similar to those we observed for the dienolate anion from 2-methylpent-2-enal, the ^{1}H NMR spectrum of which has been previously reported.[34] Additional, uncharacterized degradative products were seen to grow yet more slowly, likely from further aldol reactions between **13** and **11-Na**.

To test the degradation of poly(MOPO-*co*-IBVE), the copolymer was dissolved in $CDCl_3$ and stirred as a two-phase mixture with 3 M HCl for 7 h. After this time, complete degradation of the MOPO units to give just poly(IBVE) was indicated by ^{1}H NMR spectral analysis (Figure S39). THF SEC analysis further demonstrates loss of molar mass from 9.3 kg/mol down to 3.6 kg/mol (Table 3, entry 1; Figure 6). Importantly, if this polymer were a well-defined diblock, the M_n of the poly(IBVE) segment after degradation would be expected to be 7.7 kg/mol. This result, along with the NMR data, is consistent with MOPO being tapered into the IBVE backbone.

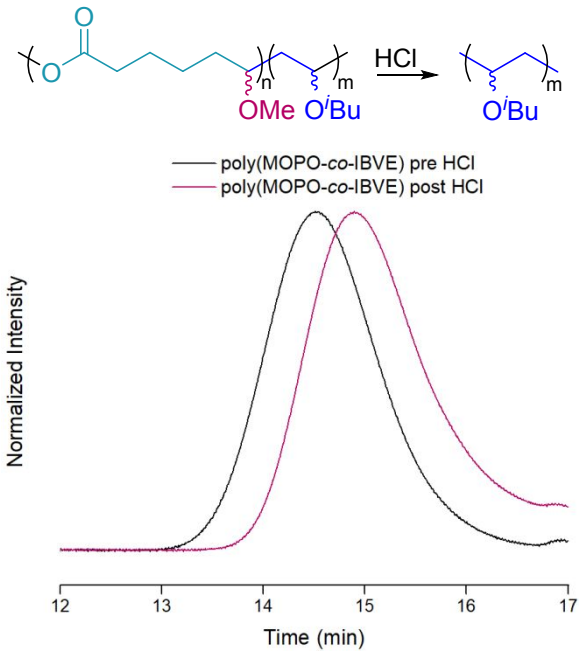

Figure 6. THF SEC trace of poly(MOPO-*co*-IBVE) with a composition of 17 mol% MOPO and 83 mol% IBVE before (M_n = 9.3 kg/mol) and after (M_n = 3.6 kg/mol) hydrolysis.

As a comparison, complete degradation of poly(MOPO) under the same conditions used to test the copolymers resulted in the corresponding aldehyde acid **11-H**, and no polymer was detected by ^{1}H NMR spectroscopy and THF SEC (Table 3, entry 2 and Figures S40–S41). Poly(IBVE) showed greater stability in HCl than either poly(MOPO-*co*-IBVE) or poly(MOPO), with polymer peaks still present in the ^{1}H NMR spectrum after 7 h and only minor loss of molar mass after 92 h (Table 3, entry 3 and Figures S42–S43). These results demonstrate the ability to incorporate MOPO with other polymers to form readily degradable copolymers.

Table 3. Degradation of poly(MOPO-*co*-IBVE), poly(MOPO), and poly(IBVE)

Entry	Polymer	Before HCl treatment		After HCl treatment	
		M_n[a] (kg/mol)	$Đ$[a]	M_n[a] (kg/mol)	$Đ$[a]
1	Poly(MOPO-*co*-IBVE)	9.3	1.48	3.6	2.22
2	Poly(MOPO)	36.8	2.30	-[b]	-[b]
3	Poly(IBVE)	17.6	1.17	14.3	1.41

[a]Determined from THF SEC relative to polystyrene standards. [b]No polymer was detected by SEC. Entries 1 and 2 were stirred as a two-phase $CDCl_3/HCl_{(aq)}$ mixture for 7 h. Entry 3 was stirred as a two-phase $CDCl_3/HCl_{(aq)}$ mixture for 92 h.

Conclusions

We demonstrated that the strained exocyclic hemiacetal ester 7-methoxyoxepan-2-one can be homo- and copolymerized quantitatively by a cationic polymerization mechanism to afford hydrolytically sensitive polyhemiacetal esters and polyvinyl ethers bearing acylacetal linkages. In the presence of strong acid as the cationic initiator the molar mass of poly(MOPO) is a function of the alkoxycarbenium lifetime rather than the initial concentration of acid. When triflic acid was used as the cationic initiator, poly(MOPO) of M_n = 20 kg/mol could be obtained reproducibly from a single monomer batch. Addition of dithiocarbamate and trithiocarbonate chain-transfer agents to the polymerization effectively lowered the M_n of poly(MOPO), consistent with a reversible deactivation polymerization mechanism. Both the homopolymer and the vinyl ether copolymer were readily degradable in hydrochloric acid via hydrolysis of the acylacetal linkages. Further investigation of chain-transfer agents will be necessary to identify those yielding the highest degree of control over the polymerization of cyclic hemiacetal esters. The high reactivity of strained cyclic hemiacetal esters makes them promising candidates for co-monomers in the polymerization of other vinyl ethers and oxiranes to yield readily degradable copolymers.

ASSOCIATED CONTENT

Supporting Information

Experimental procedures and all characterization data. This material is available free of charge via the Internet at http://pubs.acs.org.

AUTHOR INFORMATION

Corresponding Author

*Phone: 612-625-7834. E-mail: hillmyer@umn.edu. Phone: 607-254-1487. E-mail: bpf46@cornell.edu.

Author Contributions

A.E.N. and M.A.H. conceived the study. A.E.N. wrote the manuscript with input of the other authors. A.E.N., L.B., and T.J.H. carried out experimental work under the guidance of M.A.H. J.T.T. carried out the photocatalysis experiments under guidance of B.P.F. and wrote the section on photoinitiated RAFT of MOPO. G.W.F. carried out the MOPO degradation studies in acid and base under the guidance of T.R.H. and wrote the section on poly(MOPO) degradation.

Present Address

A.E.N.: Institute for Molecular Engineering, University of Chicago, Chicago, IL, 60637

Funding Sources

This work was supported by the Center for Sustainable Polymers at the University of Minnesota, a National Science Foundation supported Center for Chemical Innovation (CHE-1413862). This work made use of the Cornell Center for Materials Research Shared Facilities that are supported through the NSF MRSEC program (DMR- 1120296). B.P.F. thanks 3M for a Non-Tenured Faculty Award. This work made use of the NMR Facility at Cornell University that is supported, in part, by the NSF under the award number CHE-1531632.

Notes

The authors declare no competing financial interest.

ACKNOWLEDGMENT

The authors would like to thank Guilhem De Hoe, Dr. Thomas Vidil, and Ivan Keresztes for helpful discussions. We also acknowledge Dr. Letitia Yao and Zachary Gilbert for help with DOSY NMR kinetics experiments.

REFERENCES

1) U.S. Environmental Protection Agency. Municipal Solid Waste. https://archive.epa.gov/epawaste/nonhaz/municipal/web/html (Accessed Nov. 26, 2017).

2) World Economic Forum, Ellen MacArthur Foundation and McKinsey and Company, The New Plastics Economy Catalyzing Action; 2017; [report] https://www.ellenmacarthurfoundation.org/publications/new-plastics-economy-catalysing-action.

3) Neitzel, A. E.; Petersen, M. A.; Kokkoli, E.; Hillmyer, M. A. Divergent mechanistic avenues to an aliphatic polyesteracetal or polyester from a single cyclic esteracetal. *ACS Macro Lett.* **2014**, *3*, 1156−1160.

4) Neitzel, A. E.; Haversang, T. J.; Hillmyer, M. A. Organocatalytic cationic ring-opening polymerization of a cyclic hemiacetal ester. *Ind. Eng. Chem. Res.* **2016**, *55*, 11747−11755.

5) Cairns, S. A.; Schultheiss, A.; Shaver, M. P. A broad scope of aliphatic polyesters prepared by elimination of small molecules from sustainable 1,3-dioxolan-4-ones. *Polym. Chem.* **2017**, *8*, 2990−2996.

6) Xu, Y.; Perry, M. R.; Cairns, S. A.; Shaver, M. P. Understanding the ring-opening polymerisation of dioxolanones. *Polym. Chem.* **2019**, Advance Article, **DOI**: 10.1039/C8PY01695J.

7) Hyoi, K.; Kanazawa, A.; Aoshima, S. Cationic ring-opening co- and terpolymerizations of lactic acid-derived 1,3-dioxoloan-4-ones with oxiranes and vinyl ethers: nonhomopolymerizable monomer for degradable co- and terpolymers. *ACS Macro Lett.* **2019**, *8*, 128−133.

8) Martin, R. T.; Camargo, L. P.; Miller, S. A. Marine-degradable lactic acid. *Green Chem.* **2014**, *16*, 1768−1773.

9) Houk, K. N.; Jabbari, A.; Hall Jr, H. K.; Alemán, C. Why δ-valerolactone polymerizes and γ-butyrolactone does not. *J. Org. Chem.* **2008**, *73*, 2674−2678.

10) Neitzel, A. E. Ring-opening polymerization of cyclic hemiacetal esters for the preparation of hydrolytically and thermally degradable polymers. Ph.D. Dissertation, University of Minnesota, Minneapolis, MN, 2018.

11) Kammiyada, H.; Konishi, A.; Ouchi, M.; Sawamoto, M. Ring-expansion living cationic polymerization via reversible activation of a hemiacetal ester bond. *ACS Macro Lett.* **2013**, *2*, 531−534.

12) Kammiyada, H.; Ouchi, M.; Sawamoto, M. A convergent approach to ring polymers with narrow molecular weight distributions through post dilution in ring expansion cationic polymerization. *Polym. Chem.* **2016**, *7*, 6911-6917.

13) Kammiyada, H.; Ouchi, M.; Sawamoto, M. Expanding vinyl ether monomer repertoire for ring-expansion cationic polymerization: various cyclic polymers with tailored pendant groups. *J. Poly. Sci. Part A: Polym. Chem.* **2017**, *55*, 3082-3089.

14) Sergeev, A. G.; Hartwig, J. F. Selective, nickel-catalyzed hydrogenolysis of aryl ethers. *Science* **2011**, *332*, 439−443.

15) Schutyser, W.; van den Bosch, S.; Dijkmas, J.; Turner, S.; Meledina, M.; van Tendeloo, G.; Debecker, D. P. Selective nickel-catalyzed conversion of model and lignin-derived

phenolic compounds to cyclohexanone-based polymer building blocks. *ChemSusChem* **2015**, *8*, 1805−1818.

16) Matyjaszewski, K. Similarities and discrepancies between controlled cationic and radical polymerizations. *Ionic polymerizations and related processes* **1999**, 259–268.

17) Benneche, T.; Srtrande, P.; Oftebro, R.; Undheim, K. Pyrimidinones as reversible metaphase arresting agents. *Eur. J. Med. Chem.* **1993**, *28*, 463−472.

18) Albright, T. A.; Freeman, W. J.; Schweizer, E. E. Magnetic resonance studies. II. Investigation of phosphonium salts containing unsaturated groups by carbon-13 and phosphorus-31 nuclear magnetic resonance. *J. Am. Chem. Soc.* **1975**, *97*, 2946−2950.

19) Brzezińska, K.; Chwiałkowska, W.; Kubisa, P.; Matyjaszewski, K.; Penczek, S. Ion-trapping in cationic polymerization. *Makromol. Chem.* **1977**, *178*, 2491-2494.

20) Li, W.; Li, J.; Wu, Y.; Fuller, N.; Markus, M. A. Mechanistic pathways in CF3COOH-mediated deacetalization reactions. *J. Org. Chem.* **2010**, *75*, 1077−1086.

21) Rajabi, M.; Lanfranchi, M.; Campo, F.; Panza, L. Synthesis of a series of hydroxycarboxylic acids as standards for oxidation of nonanoic acid. *Synth. Commun.* **2014**, *44*, 1149−1154.

22) Chwiałkowska, W.; Kubisa, P.; Penczek, S. Preparation of living mono- and dicationically growing polyacetals and attempts to prepare block copolymers thereof. *Makromol. Chem.* **1982**, *183*, 753−769.

23) Alder, R. W.; Phillips, J. G. E.; Huang, L.; Huang, X. Methyltrifluoromethanesulfonate. *e-EROS Encyclopedia of Reagents for Organic Synthesis* **2005**, 1.

24) Sawamoto, M.; Okamoto, C.; Higashimura, T. Hydrogen iodide/zinc iodide: a new initiating system for living cationic polymerization of vinyl ethers at room temperature. *Macromolecules* **1987**, *20*, 2693−2697.

25) Cho, C. G.; Feit, B. A.; Webster, O. W. Cationic polymerization of isobutyl vinyl ether: livingness enhancement by dialkyl sulfides. *Macromolecules* **1990**, *23*, 1918−1923.

26) Kojima, K.; Sawamoto, M.; Higashimura, T. Living cationic polymerization of isobutyl vinyl ether by hydrogen iodide/Lewis acid initiating systems: effects of Lewis acid activators and polymerization kinetics. *Macromolecules* **1989**, *22*, 1552−1557.

27) Uchiyama, M.; Satoh, K.; Kamigaito, M. Cationic RAFT polymerization using ppm concentrations of organic acid. *Angew. Chem., Int. Ed.* **2015**, *54*, 1924–1928.

28) Sugihara, S.; Konegawa, N.; Maeda, Y. HCl·Et2O-catalyzed metal-free RAFT cationic polymerization: one-pot transformation from metal-free living cationic polymerization to RAFT radical polymerization. *Macromolecules* **2015**, *48*, 5120–5131.

29) Uchiyama, M.; Satoh, K.; Kamigaito, M. Thioether-mediated degenerative chain-transfer cationic polymerization: a simple metal-free system for living cationic polymerization. *Macromolecules* **2015**, *48*, 5533–5542.

30) McKenzie, T. G.; Fu, Q.; Uchiyama, M.; Satoh, K.; Xu, J.; Boyer, C.; Kamigaito, M.; Qiao, G. G. Beyond Traditional RAFT: Alternative activation of thiocarbonylthio compounds for controlled polymerization. *Adv. Sci.* **2016**, *3*, 1500394.

31) Kottisch, V.; Michaudel, Q.; Fors, B. P. Cationic polymerization of vinyl ethers controlled by visible light. *J. Am. Chem. Soc.* **2016**, *138*, 15535–15538.

32) Michaudel, Q.; Chauviré, T.; Kottisch, V.; Supej, M. J.; Stawiasz, K. J.; Shen, L.; Zipfel, W. R.; Abruña, H. D.; Freed, J. H.; Fors, B. P. Mechanistic insight into the photocontrolled cationic polymerization of vinyl ethers. *J. Am. Chem. Soc.* **2017**, *139*, 15530–15538.

33) Schmid, M. B.; Zeitler, K.; Gschwind, R. M. NMR investigations on the proline-catalyzed aldehyde self-condensation: Mannich mechanism, dienamine detection, and erosion of the aldol addition selectivity. *J. Org. Chem*. **2011**, *76*, 3005–3015.

34) Kloosterziel, H.; Van Drunen, J. A. A. Stereochemistry of base-catalyzed double-bond migration in inner olefins. *Recl. Trav. Chim. Pays-Bas* **1970***, 89*, 37–41.

TOC